Preparation and Characterization of Antimony-Doped Tin Dioxide Electrodes. 3. XPS and SIMS Characterization

F. Montilla,[†] E. Morallón,*[,†] A. De Battisti,[‡] S. Barison,[§] S. Daolio,[§] and J. L. Vázquez[†]

Departamento de Química Física, Universidad de Alicante, Apartado de Correos 99, Alicante, Spain E-03080, Dipartimento di Chimica, Università degli Studi di Ferrara, Via Borsari 46, 44100 Ferrara, Italy, and Istituto per l'Energetica e le Interfasi, Consiglio Nazionale delle Ricerche, Corso Stati Uniti 4, I-32157, Padova, Italy

Received: March 25, 2004; In Final Form: June 30, 2004

Several antimony- and antimony−platinum-doped tin dioxide electrodes supported on titanium have been characterized by X-ray photoelectron spectroscopy (XPS) for surface analysis and secondary-ion mass spectrometry (SIMS) for in-depth profile analysis. The surface analysis of the freshly prepared electrodes indicates that the Sb/Sn ratio in the electrode surface is similar to the nominal composition in the precursor solution, but the amount of Pt is higher than this nominal composition. The presence of platinum also produces the segregation of Sb near the electrode surface. The anodic polarization treatment of the electrode produces changes in its chemical state. The growth of a passivating hydroxide in the outer layer is the main cause of the deactivation of Ti/SnO_2−Sb electrodes. The introduction of platinum in the layer prevents the hydroxide formation and modifies the deactivation mechanism of the electrode. The growth of an isolating TiO_2 between the support and the active oxide produces the deactivation of Ti/SnO_2−Sb−Pt electrodes.

1. Introduction

Transition metal oxides supported on titanium have been used for a variety of electrochemical processes of technological interest, such as brine electrolysis, electrometallurgy, and electrochemical incineration of organics in wastewaters.[1]

The achievement of high current efficiencies in the latter application requires low catalytic activity toward the oxygen evolution reaction (OER), typically reflected by high oxygen overpotentials. Several electrodes with this property have been employed, i.e., PbO_2,[2] boron doped diamond electrodes (Si/BDD),[3,4] and SnO_2−Sb electrodes.[5−7] Antimony-doped tin dioxide supported on titanium has emerged as a new anode for the removal of organic pollutants from aqueous wastes, allowing the attainment of efficiencies higher than those of more traditional materials, such as PbO_2 and Pt.[7]

Significant drawbacks of Ti/SnO_2−Sb are, however, its low stability and short service life under OER. The service life of this kind of electrodes is determined by two key interfaces that may suffer chemical modifications during electrochemical treatments: the inner layer between the support and the active oxide and the outer interface between the active oxide and the electrolyte solution. Several mechanisms can be involved in the anode deactivation, that is, the detachment of the electrocatalyst, the dissolution of the active oxide, and the passivation of any of the key interfaces. The oxidation of the titanium substrate, for instance, produces the formation of a nonconductive TiO_2 interlayer blocking the charge transfer from the support to the oxide layer.[8] On the other hand, some chemical modification of the electrode outer surface (oxide|electrolyte interface), such as a loss of the dopant component, may produce the passivation for charge transfer to the solution.[9]

X-ray photoelectron spectroscopy (XPS) is a powerful technique extensively employed in the determination of the chemical composition and chemical state of several surfaces. This technique is surface-selective (sampling penetration depth 1−3 nm) and has been employed in the analysis of several dimensionally stable anodes (DSA) such as RuO_2 and IrO_2 supported on titanium.[10−12]

Secondary-ion mass spectrometry (SIMS) gives information about the in-depth composition and chemical state of the inner layers. This technique has been successfully used in several studies of electrodes of metallic oxides, such as the determination of the component distribution along the oxide layers, the interdiffusion phenomena between the oxide and the support, the analysis of chemical modifications suffered during electrochemical treatments, etc.[13−15]

In our previous papers, several Sb-doped SnO_2 electrodes with and without platinum have been studied regarding electrochemical and structural characterizations.[16,17] The electrochemical characterization suggests that Ti/SnO_2−Sb electrodes suffer deactivation due to the formation of a passive layer in the outer interface.[16] The introduction of platinum in the tin dioxide layer prevents the formation of this passive outer layer. Then the possible deactivation mechanism in the Ti/SnO_2−Sb−Pt electrodes could be the formation of a passive layer between the support and the active oxide. This conclusion was supported on indirect evidence such as capacitance measurements.[16] Moreover, the structural modification of the anodic deactivated electrodes was studied in part 2.[17] The deactivated oxide layer of antimony-doped SnO_2 suffers strong modification of the lattice parameters, and platinum prevents this change in the tin oxide unit cell.[17] However, X-ray techniques are not able to distinguish between the two interfaces implied in the deactivation mechanism. For that reason, a surface-sensitive technique such as XPS can inform us about the chemical shift of the outer layer. Chemical modifications across the oxide layer can be checked by SIMS profile analysis. These are the studies

* Corresponding author. E-mail: morallon@ua.es.
[†] Universidad de Alicante.
[‡] Università degli Studi di Ferrara.
[§] Consiglio Nazionale delle Ricerche.

10.1021/jp048674+ CCC: $27.50
Published on Web 09/21/2004

TABLE 1: Atomic Concentrations, Concentration Ratios, and Relative Intensity of the Peak of OH Species Related to the Peak of M−O Species of Freshly Prepared Sb-Doped and Sb−Pt-Doped SnO_2 Electrodes

	atom %				concentration ratio			rel int
	Sn	Sb	Pt	O	Sb/(Sn + Sb + Pt)	Pt/(Sn + Sb + Pt)	O/(Sn + Sb + Pt)	I_{OH}/I_{MO}
Ti/SnO_2−Sb	20	2.1		77	0.10		3.4	0.71
Ti/SnO_2−Sb−Pt (3 atom %)	16	3.9	2.5	77	0.17	0.11	3.4	0.67
Ti/SnO_2−Sb−Pt (13 atom %)	11	5.5	5.1	79	0.25	0.24	3.7	0.55

performed in the present work: these electrodes have been analyzed using techniques such as XPS and SIMS that are more sensitive to the surface. Special attention has been paid to the oxidation state of the doping atoms (Sb and Pt). In-depth profile analysis has been done using SIMS spectrometry in order to study the segregation of the different components in the oxide layer. Finally, a study has been completed about the modifications suffered after the anodic deactivation of the doped tin dioxide electrodes.

2. Experimental Section

Electrodes of tin dioxide were prepared by thermal decomposition of the salt precursor on a titanium substrate. The salt precursors were $SnCl_4 \cdot 5H_2O$ (Aldrich), $SbCl_3$ (Fluka p.a.), and H_2PtCl_6 in a mixture of ethanol (Merck p.a.) + HCl (Merck p.a.). Prior to the deposition process, the Ti support was etched during 1 h in a solution of boiling oxalic acid (10%). Ti/SnO_2−Sb electrodes were prepared using a solution containing 10% $SnCl_4 \cdot 5H_2O$ + 1% $SbCl_3$, and the electrodes containing platinum were prepared by adding to the previous solution a precursor of platinum. Two sets of electrodes were prepared by adding 0.4 wt % (3 atom %) and 2.1 wt % (13 atom %) H_2PtCl_6, respectively. The precursor solution was brushed on a Ti plate (1 × 1 × 0.05 cm), and the electrode was introduced in an oven at 400 °C for 10 min. This process was repeated 10, 20, and 30 times for attaining different film thicknesses. A final annealing was performed at 600 °C for 1 h. Details about the preparation method were described in a previous paper.[16] Three types of electrodes were prepared with the following nominal compositions: Ti/SnO_2−Sb (12 atom %), Ti/SnO_2−Sb (12 atom %)−Pt (3 atom %), and Ti/SnO_2−Sb (12 atom %)−Pt (13 atom %).

The XPS spectra have been obtained with a VG-Microtech Multilab electron spectrometer, by using Mg Kα (1253.6 eV) radiation from a twin anode source. Photoelectrons were collected at a takeoff angle of 90° into a hemispherical analyzer working in the constant energy mode at a pass energy of 50 eV. The pressure of the analysis chamber was maintained at 5 × 10^{-10} mbar. The binding energy (BE) and the Auger kinetic energy (KE) scale were regulated by setting the C 1s transition at 284.6 eV. The BE and KE values were obtained by using the Peak-fit Program implemented in the control software of the spectrometer with an accuracy of ±0.2 and ±0.3 eV, respectively.

SIMS analyses were performed by a recently updated instrument based on commercial components.[18] The analytical chamber is equipped with two primary ion sources: a mass-filtered duoplasmatron ion gun (Model DP50B by VG Fison) that generated an O_2^+ ion beam collimated to 50 μm and an electron impact ionization source IQE 12/38 by SPECS, which provided an inert gas (Ne^+ and Ar^+) ion beam. In our experiment a 6 keV O_2^+ ion beam was chosen; the projectiles were directed at an angle of incidence of 30° with respect to the surface plane for both primary ion sources, and secondary ions were measured in the normal direction to the sample surface.

A mass-energy analyzer (Model EQS1000, Hiden, UK) with high transmission 45° sector field energy and a quadrupole mass filter were used for negative- and positive-ion detection in counting mode. Lens and energy analyzer potential, quadrupole electronic control units, and the detection system were controlled via a Hiden HAL IV interface. The pressure in the chamber was typically 5 × 10^{-10} mbar. During experiments the pressure of the working gases was maintained between 3 × 10^{-9} and 5 × 10^{-9} mbar.

The ion species were identified by resolving the overlapped *m/z* signals with an isotope pattern simulation program. In-depth ion species distribution was analyzed following signals of interest as a function of bombarding time. Border effects were avoided with the electronic gating (only secondary ions coming from the central 50% of rastered area were collected).

3. Results and Discussion

3.1. Analysis of Freshly Prepared Electrodes. *3.1.1. XPS Analysis.* Figure 1 shows the complete XPS spectrum of a Ti/SnO_2−Sb electrode in which the peaks corresponding to C (surface contamination), Sn, Sb, O, and Ti can be observed. The atomic composition determined by XPS is shown in Table 1. The ratio of doping atoms, (Sb or Pt)/(Sn + Sb + Pt), and oxygen atom to the total metallic atoms O/(Sn + Sb + Pt) are also included in Table 1. The oxygen ratio is around 3.4, a value higher than the stoichiometric value for SnO_2, which is indicative of the presence of different species on the surface such as tin hydroxides $Sn(OH)_4$ or partially hydrated species.

The relative amount of Sb [Sb/(Sn + Sb + Pt)] for a Ti/SnO_2−Sb electrode is slightly lower than the nominal composition of Sb (12 atom %). However, for electrodes containing platinum the relative amount of antimony is higher than the nominal composition, possibly due to different deposition yield or to Sb enrichment on the surface by the presence of platinum in the layer. This point will be further discussed in the SIMS analysis section.

The relative amount of platinum in the surface is higher than the nominal composition. This fact can be due to either a surface enrichment with the noble metal or to a higher deposition yield

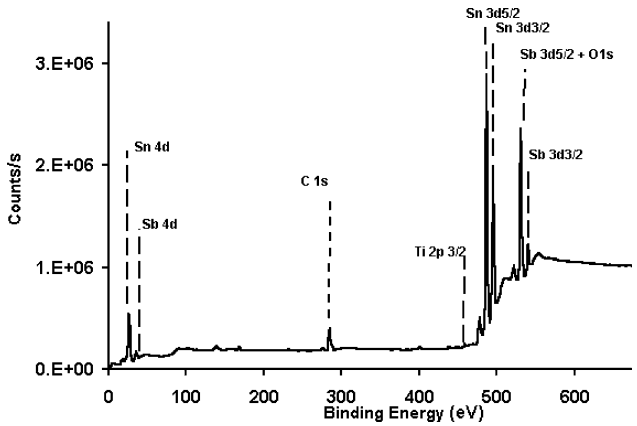

Figure 1. General XPS spectrum of freshly prepared Ti/SnO_2−Sb electrode.

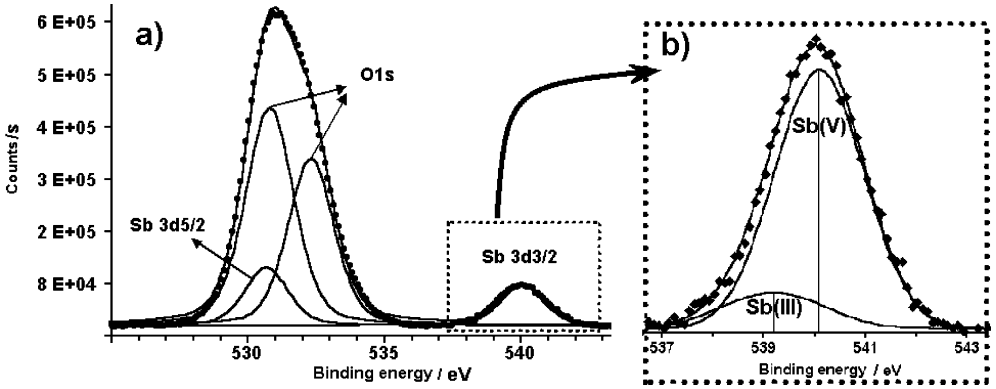

Figure 2. XPS spectrum of O 1s and Sb 3d transition region of freshly prepared Ti/SnO_2−Sb electrode.

TABLE 2: Binding Energies of Transition Levels of Several Atoms Detected in XPS Analysis of Sb-Doped and Sb−Pt-Doped SnO_2 Electrodes Freshly Prepared and Deactivated by Anodic Treatment

		binding energy (eV)	
element	transition level	freshly prepared electrodes	deactivated electrodes
Ti	$2p_{3/2}$	458.7 ± 0.2	458.8 ± 0.2
Sn	$3d_{5/2}$	487.0 ± 0.2	486.9 ± 0.2
Sb	$3d_{5/2}$	530.6 ± 0.3	530.5 ± 0.3
	$3d_{3/2}$	540.0 ± 0.2,[a] 540.4 ± 0.2[b]	540.1 ± 0.3
Pt	$4f_{7/2}$	70.8 ± 0.5	71.3 ± 0.5
	$4f_{7/2}$	72.7 ± 0.5	72.9 ± 0.5
	$4f_{7/2}$	74.7 ± 0.3	74.8 ± 0.3
O	1s	531.0 ± 0.3	530.9 ± 0.3
	1s	532.4 ± 0.4	532.3 ± 0.4

[a] Sb-doped electrodes. [b] Sb−Pt-doped electrodes.

of this metal from its precursor, with respect to the Sn and Sb precursors. Comninellis and Verseci[19] have determined that the deposition yield of SnO_2 is lower than the yield of Pt deposition from its corresponding chlorides as a consequence of the higher volatility of the tin precursor ($SnCl_4$). The distribution of the doping atoms along the oxide layer will be further discussed, making use of SIMS analysis.

The oxidation state of the elements on the electrode surface has been determined by XPS analysis. Table 2 shows the binding energies of the different transition levels for the atoms detected on the electrode surface for different freshly prepared antimony and antimony−platinum doped SnO_2 electrodes.

A small amount of titanium has been detected in all the electrodes prepared (below 1 atom %). This fact indicates migration of Ti species from the support during the thermal preparation of the electrodes at 400−600 °C.[20] The binding energy of the transition Ti $2p_{3/2}$ is 458.7 ± 0.1 eV, which is characteristic of a titanium +4 (TiO_2) oxidation state.[21]

The $3d_{5/2}$ transition peak of Sn has been analyzed for the determination of the chemical state of this element. The binding energy found in all the electrodes studied was 487 ± 0.2 eV, which agrees with a tin oxidation state of +2 or higher, probably +4, but does not allow discrimination between SnO, SnO_2, or hydroxylated species.[22] The binding energy of the Sn $3d_{5/2}$ transition is not affected by the presence of platinum in the oxide layer, which shows that the electronic structure of SnO_2 is not substantially affected by the presence of the noble metal.[23]

Special attention has been paid to the analysis of the chemical state of the doping atoms in the surface. Figure 2a shows the XPS spectrum obtained between 525 and 544 eV for a Ti/SnO_2−Sb electrode in which peaks corresponding to transitions of Sb and O atoms can be observed. The peak corresponding to the Sb $3d_{5/2}$ transition is masked by the peak of the O 1s transition. This peak can be separated from the O peaks, making use of the transition Sb $3d_{3/2}$ at higher binding energy, since the intensity ratio between both is 1.44. The other Sb transition ($3d_{3/2}$) has been employed to obtain the oxidation state of antimony (Figure 2b). Terrier et al. have developed a method for the measurement of the Sb^{5+}/Sb^{3+} ratio in antimony-doped SnO_2 layers by means of the deconvolution of this Sb $3d_{3/2}$ transition peak.[24,25] This peak (centered at 540.0 eV) can be separated into two contributions: the Gaussian line centered at 540.1 eV corresponds to antimony with an oxidation state of Sb(V), while the peak at 539.2 eV corresponds to Sb(III). Figure 2b shows the deconvolution of both peaks in the Sb $3d_{3/2}$ transition for a Ti/SnO_2−Sb electrode.

Some amount of Sb^{3+} in the surface can be detected for electrodes without platinum (around 18% of the total antimony), but the major species in all cases is Sb^{5+}. Other authors have detected the presence of Sb^{3+} on the surface and in grain boundaries of antimony-doped SnO_2 layers prepared under similar thermal conditions for Sb atomic concentrations higher than 10%.[22,24,26−28] The peak of the Sb $3d_{3/2}$ transition is centered at 540.4 eV in platinum-containing electrodes. This binding energy corresponds to Sb^{5+}; therefore no Sb^{3+} is detected on the surface, despite the amount of Sb detected being higher than 10%. Hence the presence of the noble metal on the surface promotes the complete oxidation of the Sb in the deposited layer.

The O 1s transition can be separated into two contributions (after removal of the Sb $3d_{5/2}$ peak interference, Figure 2a): a peak centered at 531.0 eV is related with oxygen directly bonded to a metal atom and characteristic of metallic oxides (M−O); the peak at higher binding energy around 532.4 eV is related with oxygen bound to metal hydroxides (M−OH) or hydrated species on the surface.[10−12,23] The ratio between OH species and M−O species (I_{OH}/I_{MO}) is shown in Table 1, and it can be calculated from the deconvolution of the O 1s peak.

The oxidation state of platinum has been also determined by XPS spectroscopy. Figure 3 shows the XPS spectrum in the region of Pt $4f_{7/2}$ transition for a Ti/SnO_2−Sb−Pt (13 atom %) electrode. The complex spectrum obtained between 66 and 82 eV can be separated into three main peaks (and three secondary peaks) corresponding to different oxidation states of platinum present in the electrode surface. The peak at lower binding energy (70.8 ± 0.5 eV) corresponds to metallic platinum. The peaks with higher binding energies are assigned to platinum oxides: Pt(II) at 72.7 ± 0.5 eV and Pt(IV) at 74.7 ± 0.3 eV.

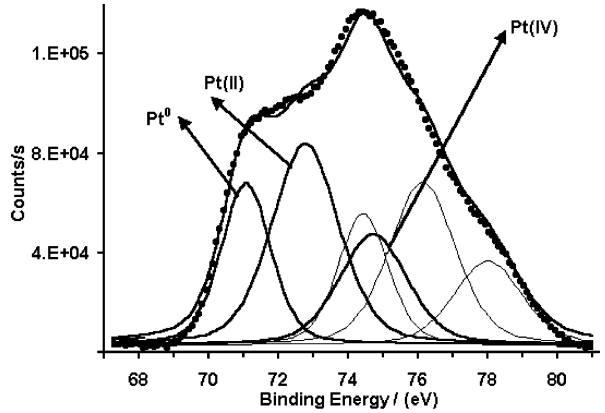

Figure 3. XPS spectrum of Pt $4f_{7/2}$ transition region of freshly prepared Ti/SnO_2-Sb electrode.

These Pt transitions can be observed in the electrodes containing platinum, but Pt(II) is the predominant species in all samples.

3.1.2. SIMS Analysis. SIMS spectrometry has been used for the detection of selected species and in-depth analysis of the chemical composition of the electroactive layers.

In all the electrodes studied some titanium has been detected on the electrode surface as detected by XPS. Titanium may reach the surface by a diffusion of ionic species coming from the metallic support during electrode preparation. Ti^+, TiO^+, TiO_2H^+, Ti_2O^+, Ti_3O^+, and several negative ions $Ti_xO_y^-$ have been the Ti species observed by SIMS. The high intensity of the titanium signals can be related either to high roughness of the electrode, to an interdiffusion phenomenon between the support and the oxide layer, or to the high Ti ion yield.[15] Several bimetallic clusters can be found, such as $SnTiO_x^+$ and $SbTiO_2^+$, indicating the possible presence of a mixed phase (i.e., solid solution) between Sb-doped SnO_2 and Ti.

Several tin species have been detected, such as Sn^+, tin oxides $Sn_xO_y^+$, and hydroxylated species $Sn_xO_yH^+$. With respect to the doping atom, antimony ions such as Sb^+ and $Sb_xO_y^+$ have been detected by this technique. In addition, several mixed clusters $SnSb^+$ and $SnSbO^+$ have been observed, which suggests the possible formation of a solid solution between Sn and Sb species. In the case of Sb−Pt-doped electrodes, several Pt ions have been detected with SIMS spectrometry, such as Pt^+, PtO^+, Pt^-, PtO^-, PtO_2^-, and mixed clusters such as $PtSn^+$ and $PtSnO^+$.

Figure 4a shows the evolution of the Sn^+ signal during the bombardment of different freshly prepared doped SnO_2 electrodes. The presence of platinum in the oxide layer produces the decrease of the ionic yield of Sn species. Figure 4b shows the evolution of Sb^+ ion along the oxide layer. While the trend of Sb^+ is similar to that followed by the Sn^+ signals for SnO_2-Sb electrodes without platinum, a significant difference can be observed in the profile for electrodes doped with platinum. An increase of the Sb signals for the electrodes of $Ti/SnO_2-Sb-Pt$ can be observed at the initial stages of the sputtering process, that is, in the outer layer of these electrodes. Figure 4c shows the ratio of the Sb^+/Sn^+ signals for the three electrodes studied. The presence of platinum in the layer influences the distribution of antimony in the layers. In the Ti/SnO_2-Sb electrode without platinum, this element is uniformly distributed along the oxide layer; the presence of platinum produces a segregation of Sb near the electrode surface. This trend is more evident when the platinum concentration increases in the electrode composition.

The distribution of platinum along the oxide layer of $Ti/SnO_2-Sb-Pt$ electrodes is shown in Figure 5. While in the

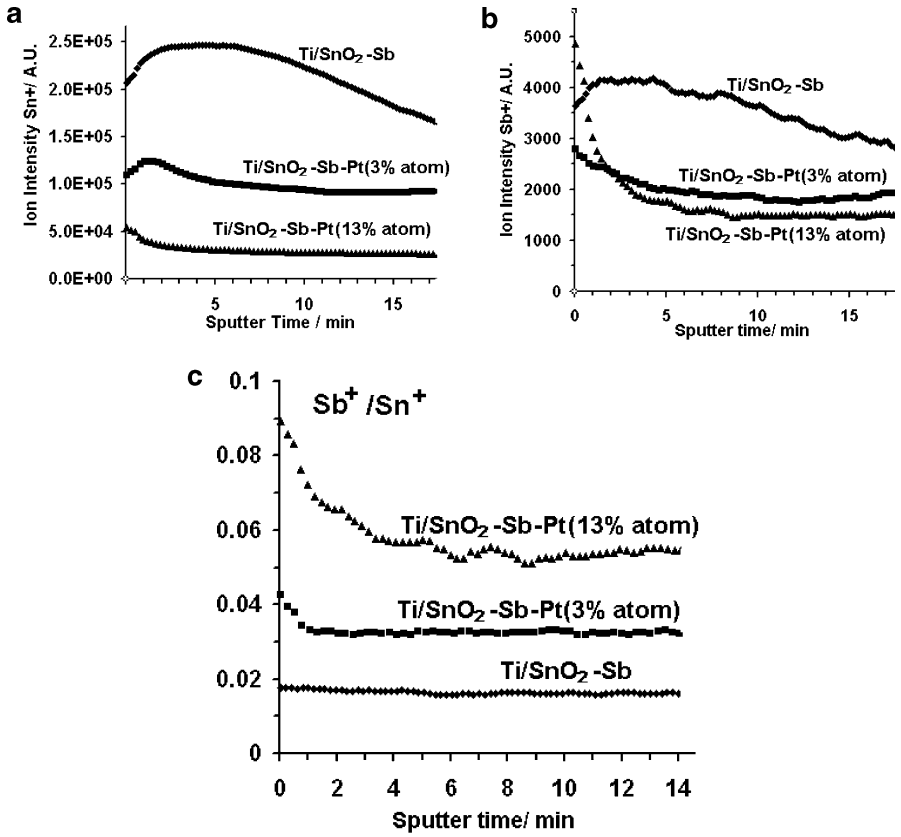

Figure 4. (a) In-depth Sn^+ ion distribution for freshly prepared Sb-doped and Sb−Pt-doped SnO_2 electrodes. Nominal composition of each electrode is shown close to its corresponding plot. (b) In-depth Sb^+ ion distribution for freshly prepared Sb-doped and Sb−Pt-doped SnO_2 electrodes. Nominal composition of each electrode is shown close to its corresponding plot. (c) Sb^+/Sn^+ relative intensity ratio as a function of sputtering time of freshly prepared Sb-doped and Sb−Pt-doped SnO_2 electrodes. Nominal composition of each electrode is shown close to its corresponding plot.

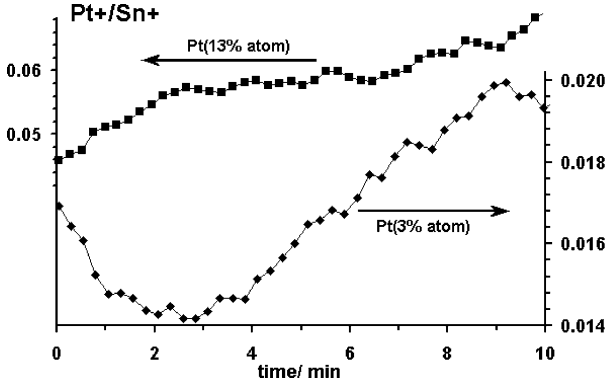

Figure 5. Pt^{+}/Sn^{+} relative intensity ratio as a function of sputtering time of freshly prepared Sb−Pt doped SnO_2 electrodes. Nominal composition of Pt for each electrode is shown close to its corresponding plot.

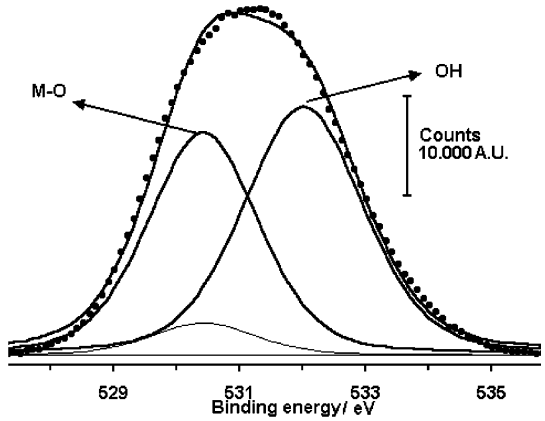

Figure 6. XPS spectrum of O 1s transition region of Ti/SnO_2−Sb electrode after anodic service life test.

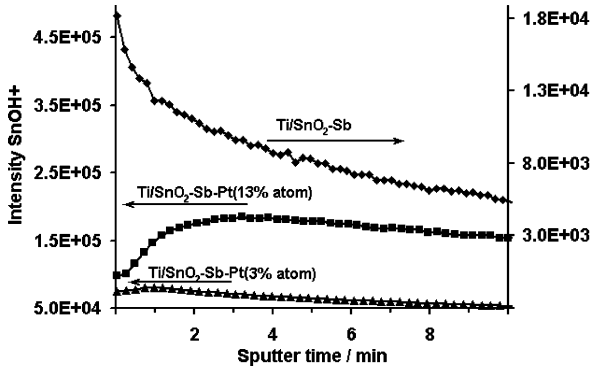

Figure 7. In-depth $SnOH^{+}$ ion distribution for Sb-doped and Sb−Pt-doped SnO_2 electrodes after anodic service life test. Nominal composition of each electrode is shown close to its corresponding plot.

electrode with 3 atom % platinum there is a slight enrichment of the platinum in the outer layer, in electrodes containing 13% platinum this element is uniformly distributed along the tin oxide film.

3.2. Analysis of Deactivated Electrodes. The service life of the electrodes prepared in this work has been checked by accelerated service life tests in the oxygen evolution reaction at a constant current of 1 A cm^{-2} in 0.5 M H_2SO_4 solution, until the total deactivation of the electrodes.[16,17] The presence of platinum in the layer increases the service life of the electrode by several orders of magnitude. The compositional aspects of the electrodes have been checked by XPS and SIMS after anodic deactivation. Table 3 shows the surface composition of deactivated electrodes measured by XPS analysis. The ratio of Sb to the total metallic atoms for the Ti/SnO_2−Sb electrodes after deactivation is similar to that for the fresh electrodes (Table 1), but a significant increase of the ratio of O to the total metallic atoms can be observed. On the other hand, a increase of the relative species of platinum on the surface is observed in electrodes containing platinum. This result could be due to the preferential dissolution or detachment of the SnO_2 deposit by the anodic treatment.

Important information can be obtained from the analysis of the O 1s transition of these electrodes. Figure 6 shows the O 1s XPS spectrum for an anodically deactivated Ti/SnO_2−Sb electrode. The O 1s XPS spectrum suffers some modifications in comparison with the O 1s XPS spectrum for a freshly prepared electrode (Figure 2). The relative intensity of the peak related with OH species (Table 3) increases to 1.24, indicating the formation of hydrated species on the surface upon anodic polarization. However, this increase is much lower for electrodes containing platinum (0.51 for deactivated Ti/SnO_2−Sb−Pt (3 atom %) and 0.75 for electrodes containing 13 atom % platinum). Therefore, the presence of platinum in the layer partially prevents the hydroxide formation in the electrode surface.

The transition Pt $4f_{7/2}$ of platinum for deactivated electrodes can be separated into three contributions, as in the case of freshly prepared electrodes: metallic Pt, Pt^{II}, and Pt^{IV} (figure not shown). However, the binding energies of these transitions are shifted toward higher values with respect to the fresh electrodes (Table 2). The transition of Pt^{0} appears at 71.3 ± 0.1 eV (a shift of +0.5 eV with respect to the fresh electrodes), the Pt^{II} transition appears at 72.9 ± 0.1 eV (shifted +0.2 eV), and the Pt^{IV} transition appears at 74.8 ± 0.1 eV (shifted +0.1 eV) for deactivated electrodes. These chemical shifts are indicative of platinum surroundings with a higher amount of electronegative species, that is, a more oxidized environment. In the same case of freshly prepared electrodes, Pt^{II} is the predominant species and is present in a higher amount in deactivated electrodes.

Figure 7 shows the SIMS profile obtained for the signal related to hydroxylated species of tin ($SnOH^{+}$) for deactivated electrodes. Significant differences can be observed between the distributions of these species along the oxide films as a function of the content of platinum. The presence of hydrated species is higher in the outer zones of the Ti/SnO_2−Sb deactivated electrode. In contrast, the hydrated species are distributed along the oxide film. The hydrated species are in higher concentration inside the bulk oxide layer.

These results indicate that the deactivation of antimony-doped tin dioxide electrodes by anodic polarization is due to the formation of a hydroxylated passive layer in the electrode surface.[29,30] However, in electrodes containing platinum the

TABLE 3: Atomic Concentrations, Concentration Ratios, and Relative Intensity of the Peak of OH Species Related to the Peak of M−O Species for Sb-Doped and Sb−Pt-Doped SnO_2 Electrodes after Anodic Service Life Tests

	atom %				concentration ratio			rel int
	Sn	Sb	Pt	O	Sb/(Sn + Sb + Pt)	Pt/(Sn + Sb + Pt)	O/(Sn + Sb + Pt)	I_{OH}/I_{MO}
Ti/SnO_2−Sb	14	1.1		83	0.07		5.3	1.24
Ti/SnO_2−Sb−Pt (3 atom %)	15	2.0	4.7	78	0.09	0.22	3.6	0.51
Ti/SnO_2−Sb−Pt (13 atom %)	10.8	2.3	6.2	80	0.12	0.32	4.1	0.75

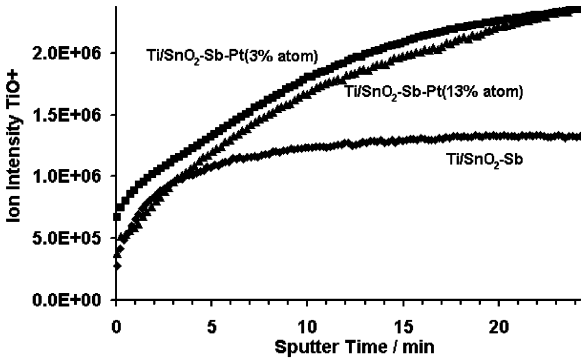

Figure 8. In-depth TiO^+ ion distribution for Sb-doped and Sb−Pt-doped SnO_2 electrodes after anodic service life test. Nominal composition of each electrode is shown close to its corresponding plot.

deactivation mechanism seems to be different, since the outer hydroxylated layer does not appear.

A possible reason for the deactivation of the SnO_2−Sb−Pt electrodes supported on titanium could be the passivation of the inner interface between the Ti and the active oxide, as a result of the growth of an insulating TiO_2 layer. Figure 8 shows the profile of the TiO^+ signal of deactivated doped SnO_2 electrodes. In the outer layer of the electrodes, the amount of Ti oxides is similar; however, as the ion beam advances along the oxide layer, the amount of TiO^+ detected is higher for deactivated Ti/SnO_2−Sb−Pt electrodes. This result is indicative of the formation to a greater extent of a TiO_2 species in electrodes that produces the passivation and deactivation of the electrode.

4. Conclusions

The surface and in-depth composition of antimony and antimony−platinum doped SnO_2 electrodes supported on titanium prepared by thermal decomposition have been studied making use of XPS (surface analysis) and SIMS (in-depth analysis) techniques.

The average amount of Sb in the electrode surface is 15 atom %, which is similar to the nominal composition of the doped SnO_2 electrodes (12 atom %). The presence of platinum in the layer produces the segregation of Sb near the electrode surface.

The amount of platinum detected by XPS in Ti/SnO_2−Sb−Pt is 2 or 3 times higher than the nominal composition. This is due to a higher efficiency of the platinum deposit with respect the SnO_2−Sb deposition. In addition, a surface enrichment of Pt with respect to the bulk composition can be observed in the Ti/SnO_2−Sb−Pt (3 atom %) electrode.

The species present on the electrode surface are Sn with a +4 oxidation state forming dioxides and hydroxides of tin. The antimony is mainly present as Sb^{5+}, but in the Ti/SnO_2−Sb electrodes some Sb^{3+} can be found in the electrode surface. In Ti/SnO_2−Sb−Pt electrodes the noble metal presents a predominant oxidation state of +2, probably PtO. In addition, some Ti^{4+} is detected in the electrode surface, which is indicative of the migration and diffusion of atoms from the support through the oxide layer, as can be confirmed by SIMS.

The electrode wearing under anodic polarization causes changes in the electrode composition. The deactivation of Ti/SnO_2−Sb electrodes is mainly due to the formation of a passivating layer (probably an electronic insulator hydroxide) in the electrode outer layer in contact with the electrolyte solution. However, the passivating layer allows ionic charge transfer and therefore capacitance phenomena are not impeded, in agreement with electrochemical results obtained in a previous paper.[16]

The mechanism for the deactivation of platinum-containing electrodes is different, since platinum prevents hydroxide formation. The platinum of doped SnO_2 electrodes suffers bulk oxidation during anodic polarization treatments, and a drop in the platinum particle size has been detected by means of XRD.[17] Furthermore, deactivated Ti/SnO_2−Sb−Pt electrodes present a higher proportion of titanium oxides distributed across the active oxide layer. The formation of a passivating TiO_2 layer between the support and the oxide layer seems to be the most probable mechanism for the electrode deactivation. Therefore, the capacitative currents in deactivated Ti/SnO_2−Sb−Pt electrodes must be decreased as previously checked by electrochemical methods.[16]

Acknowledgment. The authors thank Ministerio de Ciencia y Tecnología and FEDER (MAT 2001-1007) for financial support.

References and Notes

(1) Trasatti, S. *Electrochim. Acta* **2000**, *45* (15−16), 2377−2385.
(2) Johnson, D. C.; Feng, J.; Houk, L. L. *Electrochim. Acta* **2000**, *46* (2−3), 323−330.
(3) Montilla, F.; Michaud, P. A.; Morallon, E.; Vazquez, J. L.; Comninellis, C. *Electrochim. Acta* **2002**, *47* (21), 3509−3513.
(4) Rodrigo, M. A.; Michaud, P. A.; Duo, I.; Panizza, M.; Cerisola, G.; Comninellis, C. *J. Electrochem. Soc.* **2001**, *148* (5), D60−D64.
(5) Comninellis, C.; Pulgarin, C. *J. Appl. Electrochem.* **1993**, *23* (2), 108−112.
(6) Grimm, J. H.; Bessarabov, D. G.; Simon, U.; Sanderson, R. D. *J. Appl. Electrochem.* **2000**, *30* (3), 293−302.
(7) Stucki, S.; Kotz, R.; Carcer, B.; Suter, W. *J. Appl. Electrochem.* **1991**, *21* (2), 99−104.
(8) Martelli, G. N.; Ornelas, R.; Faita, G. *Electrochim. Acta* **1994**, *39* (11−12), 1551−1558.
(9) Beck, F. *Electrochim. Acta* **1989**, *34* (6), 811−822.
(10) Kodintsev, I. M.; Trasatti, S.; Rubel, M.; Wieckowski, A.; Kaufher, N. *Langmuir* **1992**, *8* (1), 283−290.
(11) Endo, K.; Katayama, Y.; Miura, T.; Kishi, T. *J. Appl. Electrochem.* **2002**, *32* (2), 173−178.
(12) da Silva, L. A.; Alves, V. A.; de Castro, S. C.; Boodts, J. F. C. *Colloids Surf., A: Physicochem. Eng. Asp.* **2000**, *170* (2−3), 119−126.
(13) Barison, S.; De Battisti, A.; Fabrizio, M.; Daolio, S.; Piccirillo, C. *Rapid Commun. Mass Spectrom.* **2000**, *14* (23), 2165−2169.
(14) Daolio, S.; Facchin, B.; Pagura, C.; Debattisti, A.; Gelosi, S. *Inorg. Chim. Acta* **1995**, *235* (1−2), 381−390.
(15) Gaidi, M.; Hazemann, J. L.; Matko, I.; Chenevier, B.; Rumyantseva, M.; Gaskov, A.; Labeau, M. *J. Electrochem. Soc.* **2000**, *147* (8), 3131−3138.
(16) Montilla, F.; Morallon, E.; De Battisti, A.; Vazquez, J. L. *J. Phys. Chem. B* **2004**, *108*, 5036−5043.
(17) Montilla, F.; Morallon, E.; De Battisti, A.; Benedetti, A.; Yamashita, H.; Vazquez, J. L. *J. Phys. Chem. B* **2004**, *108*, 5044−5050.
(18) Tolstoguzov, A.; Daolio, S.; Greenwood, C. L. *Int. J. Mass Spectrom.* **2002**, *214* (3), 327−337.
(19) Comninellis, C.; Vercesi, G. P. *J. Appl. Electrochem.* **1991**, *21* (2), 136−142.
(20) De Battisti, A.; Brina, R.; Gavelli, G.; Benedetti, A.; Fagherazzi, G. *J. Electroanal. Chem.* **1986**, *200* (1−2), 93−104.
(21) Hopfengartner, G.; Borgmann, D.; Rademacher, I.; Wedler, G.; Hums, E.; Spitznagel, G. W. *J. Electron Spectrosc. Relat. Phenom.* **1993**, *63* (2), 91−116.
(22) Hoflund, G. B.; Grogan, A. L.; Asbury, D. A.; Schryer, D. R. *Thin Solid Films* **1989**, *169* (1), 69−77.
(23) Liu, W.; Cao, X. P.; Zhu, Y. F.; Cao, L. L. *Sens. Actuators, B: Chem.* **2000**, *66* (1−3), 219−221.
(24) Terrier, C.; Chatelon, J. P.; Roger, J. A.; Berjoan, R.; Dubois, C. *J. Sol-Gel Sci. Technol.* **1997**, *10* (1), 75−81.
(25) Terrier, C.; Chatelon, J. P.; Berjoan, R.; Roger, J. A. *Thin Solid Films* **1995**, *263* (1), 37−41.
(26) Nutz, T.; Haase, M. *J. Phys. Chem. B* **2000**, *104* (35), 8430−8437.
(27) Shanthi, S.; Subramanian, C.; Ramasamy, P. *J. Cryst. Growth* **1999**, *197* (4), 858−864.
(28) Terrier, C.; Chatelon, J. P.; Roger, J. A. *Thin Solid Films* **1997**, *295* (1−2), 95−100.
(29) Kotz, R.; Stucki, S.; Carcer, B. *J. Appl. Electrochem.* **1991**, *21* (1), 14−20.
(30) Vicent, F.; Morallon, E.; Quijada, C.; Vazquez, J. L.; Aldaz, A.; Cases, F. *J. Appl. Electrochem.* **1998**, *28* (6), 607−612.